FLEXIBLE AND TRANSPARENT pH MONITORING SYSTEM WITH NFC COMMUNICATION FOR WOUND MONITORING APPLICATIONS

Rahim Rahimi, Uriel Brener, Manuel Ochoa, and Babak Ziaie
Birck Nanotechnology Center, Purdue University, West Lafayette, IN, USA
School of Electrical and Computer Engineering, Purdue University, IN, USA

ABSTRACT

This paper reports on a non-invasive, flexible, and wireless pH sensing system for monitoring wound healing progress and identifying the possibility of infection at an early stage. The device consists of a disposable, flexible pH sensor interfaced with a custom-designed, flexible, battery-less and reusable wireless (13.5 MHz, near field communication) data transmitting platform. The sensing electrodes are fabricated by low-cost direct laser scribing of ITO films, resulting in optically transparent sensors which allows for visual inspection of the wound. The sensor accurately measures a physiologically relevant range of pH 4–10 with an average sensitivity of −55 mV/pH.

INTRODUCTION

Standard practice in wound management today still relies mainly on subjective 20th century techniques, with healing assessment relying primarily on visual inspection, and treatment consisting of frequent changes of the wound dressing [1]. Changing the dressing too frequently, however, can pose detriments to wound healing since the wound healing process is disturbed, further increasing the cost and resources required for the therapy[2], [3]. Although some cases report successful timely healing of wound via such techniques, many others do not. Unnecessary dressing changes can arise since visual inspection is subjective and cannot always provide correct insight about the status of the wound. Prompt detection of improper wound healing can effectively help the healthcare practitioner to properly adjust the treatment to prevent acute wounds from becoming chronic (which would result in a much higher treatment complication and risk of developing infections).

One way to aid detection is by observing specific physiological parameters, such as pH. Under normal physiological conditions the skin has a low pH value of 4-6 due to the amino acids and fatty acid products secreted by the keratinocyte layer in the skin[4]. The low pH is beneficial to humans, since it helps to counteract microbial colonization from many human-pathogenic microorganisms which require a more alkaline environment for growth. Several clinical studies have shown that the body uses a similar defense strategy to reduce the bacterial colonization in wounds [5]. In healing acute wounds, the wound is first invaded by neutrophils to combat bacteria and the pH reduces to an acidic state of pH 4-6 as the healing progresses. However, in chronic wounds, the wound environment is more alkaline (within the range of pH 7.15 to 8.9), making it susceptible to different infections such as staphylococcus [6]. Some clinical studies have also shown that high pH levels in the wound are correlated to an increase in the biofilm formation on the wound[7]. In such cases the wound will not heal and antibiotics therapy and surgical intervention is inevitable. Due to these observations, numerous reports have suggested that monitoring the pH of the wound milieu can provide favorable insight for earlier identification of non-healing wounds and help the implementation of more effective treatment strategies [8].

Most of the pH measurements conducted by aforementioned clinical studies have used conventional flat glass membrane pH probes that can also cause further disruption to the wound tissue. In addition, these measurements require the removal of the wound dressing and cannot provide wireless reading through the dressing. These drawbacks urge the need and development of low-cost noninvasive pH monitoring systems that can be easily integrated into typical wound dressings. Among the different pH measurement approaches, potentiometric sensing is one of the most compelling methods [9]. Although researchers have recently developed pH sensing devices which can be potentially integrated into wound dressings, they are often fabricated using high-cost clean-room processes, which typically a complex and expensive readout system (network analyzer and optical spectrometer), that makes them impractical for clinical use[10]–[12]. The ability to make more economical, optically transparent sensors with simple wireless read-out methods that take advantage of today's smartphone ubiquity can significantly advance the care and management with chronic wounds.

In this work, we present a practical, low-cost solution that consists of a disposable sensor module which is fabricated by laser scrubbing commercial indium tin oxide (ITO) films (for optical transparency to observe the

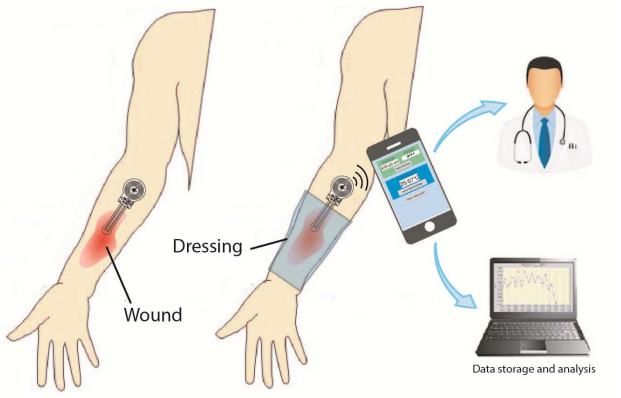

Figure 1: Schematic of the flexible wireless wound pH monitoring system utilizing NFC communication.

wound bed) interfaced with a reusable flexible potentiostat circuit with wireless near field communication (NFC). Figure 1 shows an illustration of the wireless pH monitoring system. The flexibility of the sensor and circuits allows its comfortable interface to the patient's skin. The interface operates at 13.56 MHz frequency (ISO15693) radio-frequency identification (RFID) standard that is also compatible with Android smart phones with NFC interface. The data between the pH sensing platform and the reader (e.g., smart phone) is simply transferred by bringing the reader within 4 cm proximity of the NFC tag. The communication is based on a battery-less magnetic induction between two loop antennas located within the reader and tag, effectively forming an air-core transformer.

FABRICATION

pH sensor

The sensors consist of a working electrode and reference electrode. The electrical potential across the two electrodes is a function of the concentration of H^+ ions in the analytic solution. A commercial PET flexible substrate with an ITO coating was purchased from Sigma Aldrich, and was used without further modification to serve as the transparent substrate and interconnections. The process of laser scribing and screen printing the potentiometric sensors are described in detail in Figure 2a.

The ITO film was patterned by laser-scribing using a commercial laser engraver system (Universal Laser Systems, Inc., Scottsdale, AZ) at a power and speed of 15% and 10% (out of a maximum of 75 W). The controlled laser machining process ablated the conductive ITO coating on the PET substrate, leaving behind an isolated array of transparent and flexible interconnections. To prevent shorting and crosstalk of the interconnections in the analytic solution, a transparent UV-curable adhesive (Henkel Loctite® 3105) was screen printed onto the conductive traces to define the active area and contact pads of the electrodes. The insulator was cured under UV light for 10 min. Thereafter, to define the reference electrode, a silver overlaid layer was screen printed on one of the ITO electrodes. The screen printing stencil for this process was prepared by laser cutting adhesive tape (3M® MagicTape™) at a power and speed of 20% and 10%. The tape stencil was attached to the ITO film and silver ink (118-09, CreativeMaterials, Ayer, MA) was screen printed. The ink was then allowed to cure at 70°C for 30min, and subsequently, the tape was peeled off. The silver electrode was then electrochemically chloridized in order to create the Ag/AgCl layer for the reference electrode. The chloridization process was performed by using a constant current density of 4 mA/cm^2 across the silver electrode and a Pt electrode in a 1 M NaCl solution for 5 min, forming a uniform grey layer of AgCl on the reference electrode. The electrode was then rinsed with DI water and blow-dried using nitrogen gas. The H^+ ion-selective membrane on the working electrode was prepared by electropolymerization of aniline (into polyaniline, PANI) on the pre-defined ITO areas using a three electrode system (BASi Epsilon Potentiostat, Bioanalytical Systems Inc.). In this system Pt wire was used as a counter electrode Ag/AgCl as a reference electrode and the ITO as the working electrode. The polymerization was performed at a constant potential of 0.8 V versus Ag/AgCl in a solution of 0.1 M aniline with 1 M HCl for 2 min, forming a translucent green coating of PANI on the ITO electrode. The thickness of the deposited polymer can be controlled with electropolymerization time. After the polymerization the electrodes were rinsed with DI water and blow-dried with nitrogen.

Next, the reference electrolyte was completed with a solid-state reference membrane. The solid-state membrane was prepared by mixing fine KCl powder with UV-curable adhesive (Henkel Loctite® 3105) and drop casted on to the Ag/AgCl electrode. The mixture was cured under UV light for 10 min. During the UV exposure, the PANI film on the working electrode was protected with an aluminum film cover. After the complete curing of the reference membrane, the protective layer was removed and the sensor was ready to use.

Electronic readout

The NFC interface circuit was fabricated on a commercial flexible polyimide sheet (PI) with copper laminated on both sides. The circuit was patterned using photolithography and the exposed copper was wet etched (CE-200, Transene). Next, the NFC transponder microchip (SL13 from AMS) and the surface mount buffer components were soldered onto the flexible PCB. PDMS pre-polymer (Dow Corning Sylgard® 184, 10:1 ratio) was then prepared and degassed under vacuum. The PDMS pre-polymer was poured onto the circuit and cured

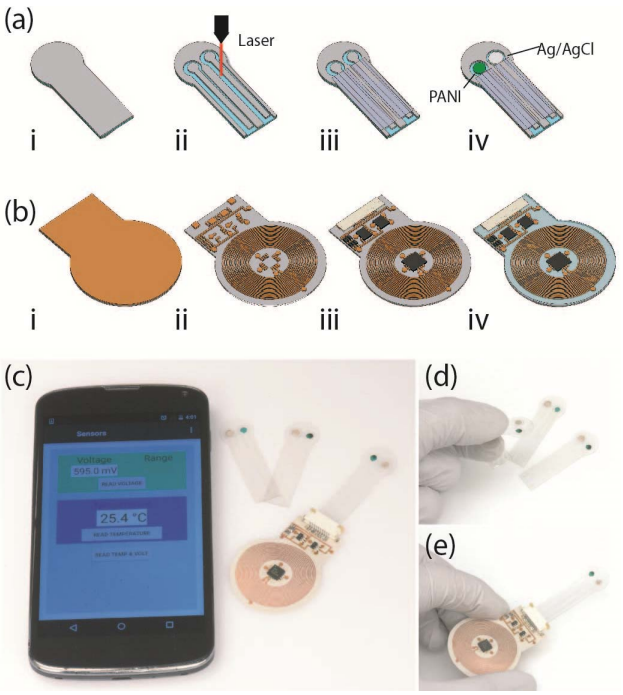

Figure 2: Fabrication process of (a) pH sensor on ITO film and (b) flexible battery less NFC module (c) photograph of completed wireless pH monitoring device and smartphone interface, images illustrating the flexibility of the (d) sensor and (e) wireless NFC module.

at 70°C for 2 hours, forming a ~500 µm-thick layer of passivation. The low power analog buffer circuit (AD8603, Analog Devices Inc.) was designed to from dual-operational amplifiers with ultra-low input bias current.

RESULT AND DISCUSSION

The laser ablated area is a result of a series of partly-overlapped single laser pluses. The optical energy delivered by the laser melts and evaporates some of the material from the surface of the film. This amount can be controlled by the laser scanning speed and the intensity. Lower intensity (or higher scanning speed) can result in partial removal of the ITO. Whereas, higher intensity (or lower scanning speed) results in deep material removal and cutting through the PET substrate. Figure 3a shows SEM image of a single laser ablated trench into the ITO film with an average width of 90 µm using the optimized laser setting (power and speed of 15% and 10%) that could be achieved with our laser machine.

To investigate the distribution of indium on the surface, the samples were further studied by EDS element mapping. The red and green colored areas shown in Figure 3b, c correspond to the existence of indium and tin elements in the material. The blue colored areas shows the presents of oxygen of the surface of the film. The clear difference color contrast in the laser ablated area shows the effective removal of the conductive ITO layer from the surface of the PET film. The oxygen present in the laser ablated trench is due to the presence of oxygen in the chemical structure of the PET substrate. Figure 3b shows the EDS spectra that was carried out along the lines on the laser ablated surface and pristine ITO film. EDX spectrum pristine ITO film exhibits a strong intensity peak at 3.28 keV, which is the characteristic of indium element, and a smaller peak at 3.44 keV that is associated with tin. The percentage of elementals on ITO the films is as follows: Sn: 4.54%, In: 4.15%, O: 37.85%, and C: 53.46%. The excess carbon and oxygen are from the polymeric PET substrate. The spectra shows complete removal of the indium and tin elemental peaks after the laser ablation.

Figure 4 shows the % optical transmittance for the different films in buffer solutions of pH 4 and 10. The UV spectrum shows the optical transparency of the ITO film before and after laser ablation in different pH solutions. However, as shown in the inset, the electrodeposited PANI exhibits a very distinguishable color change in different pH buffers (green in pH 4 and blue in pH 10). At higher acidic solutions the polyaniline film is converted to the green color emeraldine salt phase, which results in an increase in intensity of the peak at higher wavelength (~820 nm) of the optical spectra. However, in an alkaline medium (pH = 10) the spectrum exhibits at peak at ~600 nm, which is explained by the transformation of polyaniline into emeraldine base with a blue color.

The sensitivity of the pH sensor was elaluated by measuring the potential difference between the PANI working and Ag/AgCl reference electrodes at pH values in the physiological relevant range of pH 4 – pH 10.

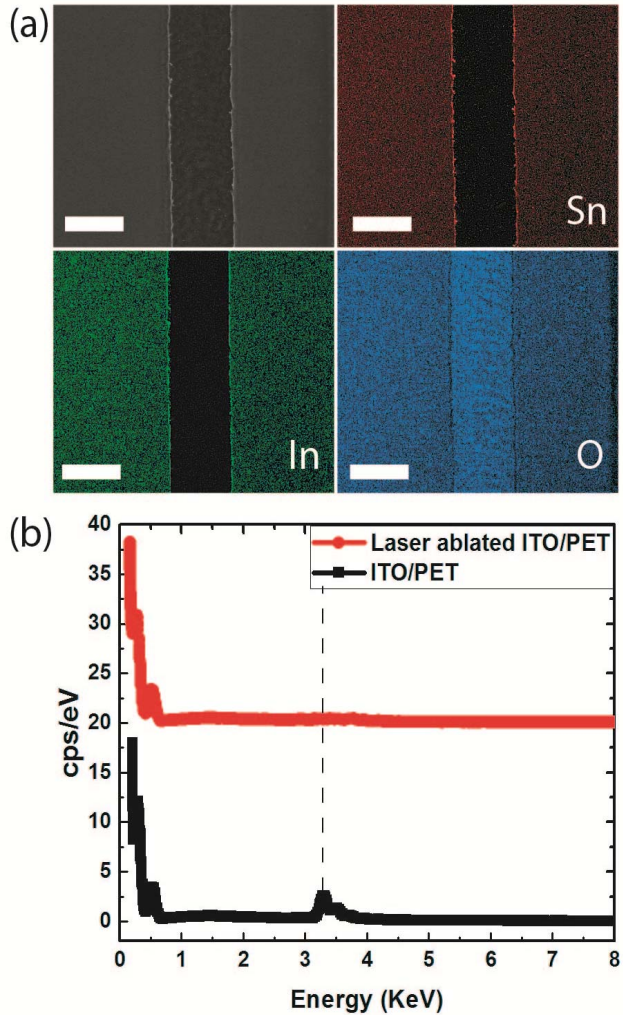

Figure 3: (a) EDX color mapping of Sn (red), In (green) and O (blue) on the ITO film after laser scrubbing with CO_2 beam, all scale bars are 100 µm, (b) EDS spectra collected from the surface ITO film before and after laser scrubbing.

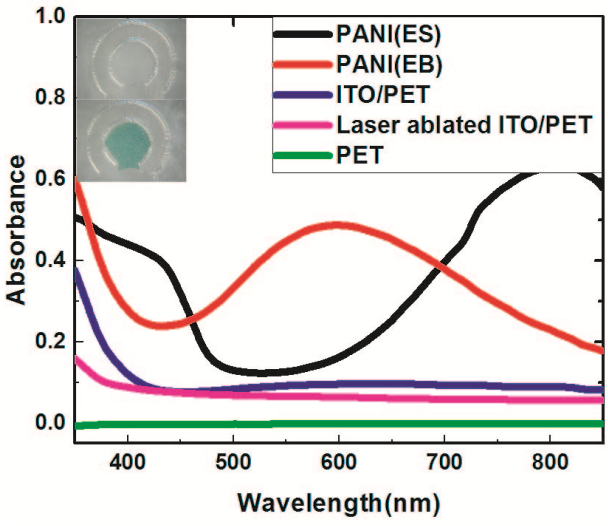

Figure 4: UV-Vis. Spectra of different layers of the pH sensor in the range of 300–900 nm, inset shows the electropolymerized polyaniline emeraldine salt (green) onto the ITO film.

Figure 5a shows the fast response of less than 28 s for increasing and decreasing pH steps, with excellent repeatability. Figure 5b shows the stable potential values obtained from the cyclic titration measurements with respect to pH. The sensors exhibits a linear Nernstian response of -55 mV/pH with a correlation coefficient r^2=0.985 across the range of pH 4-10. For wound monitoring applications, it is essential that the sensor maintains its performance under different mechanical deformations. Therefore, in order to assess the reliability the pH sensors performance was tested on a series of curved surfaces that had various curvatures. The bending test shows less than ±3 mV change in the sensitivity of the sensors and mechanical deformation has minimal affect the performance of the sensor, Figure 5b.

CONCLUSION

We have designed and characterized a highly flexible and a low-cost pH sensing system with reusable wireless module that can be used for monitoring wound healing progress. The device consists of a disposable flexible pH sensor that is interfaced with a custom-designed RFID transponder. The pH sensor fabrication process utilizes laser ablation of commercial ITO films to create flexible and transparent electrodes. The wireless module enables a wireless pH reading with NFC enabled smartphones. The pH sensors were characterized in buffer solutions of pH 4 to 10 and showed linear sensitivity of -55 mV/pH with stable performance under mechanical bending. Additionally, the wireless sensing platform can be expanded to other potentiometric sensors that can used for various ions such as sodium and potassium in the wound environment.

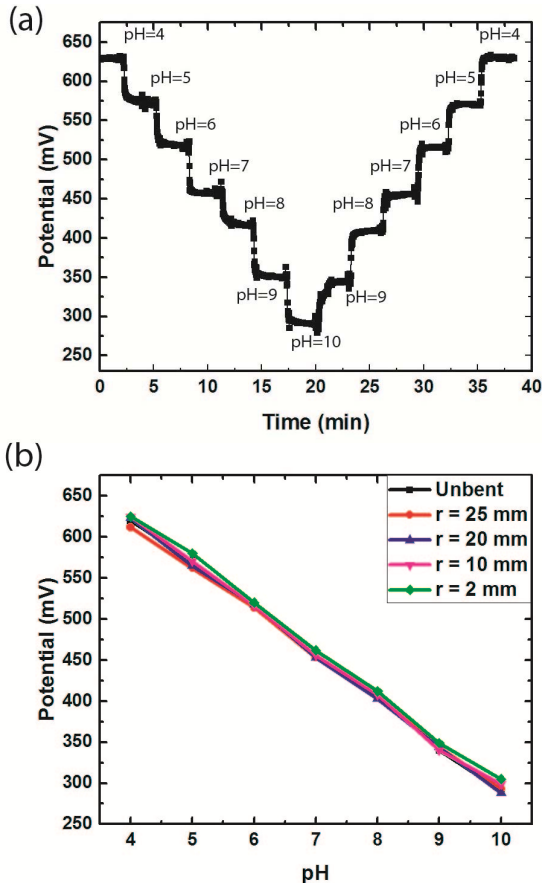

Figure 5. (a) Stability and repeatability of the pH sensor from pH 4 to 10, (b) EMF vs. pH with and without mechanical bending.

ACKNOWLEDGEMENTS

The authors thank the staff of the Birck Nanotechnology Center for their support. Funding for this project was provided in part by NextFlex PC 1.0.

REFERENCES

[1] J. E. Grey, "Wound assessment," *Bmj*, vol. 332, no. 7536, pp. 285–288, 2006.

[2] A. Mclister, J. Mchugh, J. Cundell, and J. Davis, "New Developments in Smart Bandage Technologies for Wound Diagnostics," pp. 5732–5737, 2016.

[3] M. J. Farrow, I. S. Hunter, and P. Connolly, "Developing a Real Time Sensing System to Monitor Bacteria in Wound Dressings," pp. 171–188, 2012.

[4] S. Schreml, R. M. Szeimies, S. Karrer, J. Heinlin, M. Landthaler, and P. Babilas, "The impact of the pH value on skin integrity and cutaneous wound healing," *J. Eur. Acad. Dermatology Venereol.*, vol. 24, no. 4, pp. 373–378, 2010.

[5] S. L. Percival, S. McCarty, J. a Hunt, and E. J. Woods, "The effects of pH on wound healing, biofilms, and antimicrobial efficacy.," *Wound Repair Regen.*, vol. 22, no. 2, pp. 174–86, 2014.

[6] L. A. Schneider, A. Korber, S. Grabbe, and J. Dissemond, "Influence of pH on wound-healing: A new perspective for wound-therapy?," *Arch. Dermatol. Res.*, vol. 298, no. 9, pp. 413–420, 2007.

[7] E. M. Jones, C. A. Cochrane, and S. L. Percival, "The Effect of pH on the Extracellular Matrix and Biofilms.," *Adv. wound care*, vol. 4, no. 7, pp. 431–439, 2015.

[8] M. Ochoa, R. Rahimi, and B. Ziaie, "Flexible sensors for chronic wound management.," *IEEE Rev. Biomed. Eng.*, vol. 7, pp. 73–86, Jan. 2014.

[9] R. Rahimi, M. Ochoa, T. Parupudi, X. Zhao, I. K. Yazdi, M. R. Dokmeci, A. Tamayol, A. Khademhosseini, and B. Ziaie, "A low-cost flexible pH sensor array for wound assessment," *Sensors Actuators, B Chem.*, vol. 229, pp. 609–617, 2016.

[10] S. Pasche, S. Angeloni, R. Ischer, M. Liley, J. Luprano, and G. Voirin, "Wearable Biosensors for Monitoring Wound Healing," *Adv. Sci. Technol.*, vol. 57, no. September, pp. 80–87, 2008.

[11] R. Sheybani and A. Shukla, "Highly Sensitive Label-Free Dual Sensor Array for Rapid Detection of Wound Bacteria," *Biosens. Bioelectron.*, no. October, pp. 1–9, 2016.

[12] V. Sridhar and K. Takahata, "A hydrogel-based passive wireless sensor using a flex-circuit inductive transducer," *Sensors Actuators A Phys.*, vol. 155, no. 1, pp. 58–65, Oct. 2009.

CONTACT

*B. Ziaie, tel: +1-765-494-0725; bziaie@purdue.edu